Chemical Science

ROYAL SOCIETY OF CHEMISTRY

EDGE ARTICLE

View Article Online
View Journal | View Issue

Cite this: *Chem. Sci.*, 2024, **15**, 13676

All publication charges for this article have been paid for by the Royal Society of Chemistry

Received 27th May 2024
Accepted 23rd July 2024

DOI: 10.1039/d4sc03465a

rsc.li/chemical-science

Prediction of the ground state for indenofluorene-type systems with Clar's π-sextet model†

Gibu George, [a] Anton J. Stasyuk *[abc] and Miquel Solà *[a]

This study introduces the Ground State Stability (GSS) rule that allows predicting the nature of the ground state of indenofluorene (**IF**)-type systems from the simple counting of the Clar's π-sextets in the closed- and open-shell configurations. The **IF**-type system exhibits a triplet ground state when acquiring double or more the number of Clar's π-sextets in the open-shell form relative to the closed-shell form; otherwise, it assumes an open-shell singlet ground state. Performed state-of-the-art DFT calculations and analysis of aromaticity for the systems of interest validate the effectiveness of the proposed rule. We demonstrate that aromaticity plays the most crucial role in determining the ground electronic state for such polycyclic hydrocarbons. The simplicity of the GSS rule makes it a robust strategy for identifying promising systems in the development of indenofluorene-type materials.

Introduction

Conjugated polycyclic hydrocarbons (CPHs) have gained considerable interest due to their versatile applications in optoelectronic devices,[1–4] organic spintronics[5–8] and semiconductors,[9] as well as energy storage devices.[10,11] The unique photophysical properties of CPHs make them a promising solution not only in functional materials but also found to be fundamentally important for providing insights into chemical properties such as the open-shell radical character and aromaticity.[12–15] Among such CPHs conjugated indenofluorenes (**IF**s) possess one of the most interesting topologies of delocalized π-electrons with different types of behavior (aromatic/antiaromatic) and ground state electronic structure (biradical/quinoidal).[16,17] They exhibit a 6–5–6–5–6 ring architecture, which is obtained by a fusion of the indene unit to various positions of the fluorene unit. Since 2010 all five possible **IF** regioisomers have been intensively studied by Haley's[18–20] and Tobe's[21,22] group (structures **1–5** in, Fig. 1).

In 1986, Montgomery and co-workers studied classical Chichibabin's hydrocarbon and demonstrated that diradical behavior of such a system can be explained by the regaining of two aromatic Clar's π-sextets[23,24] at the expense of a C=C double bond (**6**, **6′**).[25] More recently, Escayola *et al.*[26] studied the dependence of the nature of the ground state (closed-shell (CS) quinoidal structure *vs.* open-shell (OS) aromatic structure) in Chichibabin's hydrocarbons as a function of the elongation of the π-system and the exocyclic substituents. Similarly to Chichibabin's hydrocarbon, the **IF**s have the potential to re-aromatize the quinoidal motif leading to an OS structure that is in resonance with the CS quinoidal structure. It has been shown that structures **1** and **2** depicted in Fig. 1 exhibit a greater y_0 value (a measure of the diradical character, calculated by the Yamaguchi scheme,[27] see computational details in ESI†) than **3**, **4**, and **5**, and is mainly associated with the recovery of a larger number of the Clar's π-sextets in the OS form than the CS quinoid form.[28] Moreover, the higher diradical character for structures **1** and **2** as compared to **3**, **4**, and **5** can be associated in part with the pro-aromatic quinodimethane framework. Both **1** and **2** have a *meta*-quinodimethane (*m*-QDM) subunit (highlighted with bold red lines in Fig. 1), in contrast to the **3** with

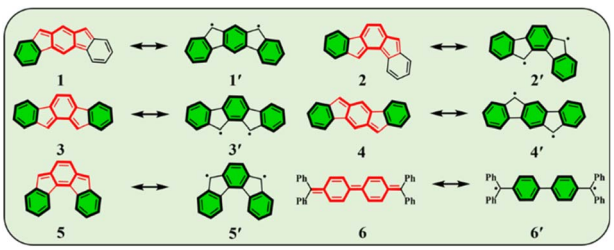

Fig. 1 Resonance structures of considered **IF**s with closed-shell (CS) and open-shell (OS) electronic nature. Structure **1** (indeno[2,1-*b*]fluorene), **2** (indeno[1,2-*a*]fluorene), **3** (indeno[2,1-*a*]fluorene), **4** (indeno[1,2-*b*]fluorene), and **5** (indeno[2,1-*c*]fluorene) are represented in the CS form, while **1′**, **2′**, **3′**, **4′**, and **5′** denote their respective OS forms. Structures **6** and **6′** are Lewis structures of Chichibabin's hydrocarbon in CS and OS forms, respectively.

[a]*Institut de Química Computacional i Catàlisi, Departament de Química, Universitat de Girona, C/Maria Aurèlia Capmany 69, 17003 Girona, Catalonia, Spain. E-mail: miquel.sola@udg.edu; antony.stasuk@gmail.com*

[b]*Faculty of Chemistry, University of Warsaw, Pasteura 1, 02-093 Warsaw, Poland*

[c]*Departament de Farmàcia i Tecnologia Farmacèutica, i Fisicoquímica, Facultat de Farmàcia i Ciències de l'Alimentació, Institut de Química Teòrica i Computacional (IQTCUB), Universitat de Barcelona (UB), Av. Joan XXIII 27-31, Barcelona, Spain*

† Electronic supplementary information (ESI) available. See DOI: https://doi.org/10.1039/d4sc03465a

ortho-quinodimethane (*o*-QDM) or **4** and **5** with *para*-quinodimethane (*p*-QDM) framework (Fig. 1).[20]

Diradical species in an open-shell form can exist in two forms, as either the OS singlet or a triplet state. Due to the dynamic spin polarization, π-diradicals[29] usually exist as OS singlets in the electronic ground state and have low-lying triplet excited states.[30] **IF**'s have been subjected to several structural modifications aiming to tune their optical and magnetic properties:[31,32] (i) a longitudinal extension of the indacene π-conjugated core (by replacing the central benzene ring of **IF** to naphthalene or anthracene units producing fluorenofluorene (**FF**)[33–35] and diindenoanthracene (**DIAn**)[36]) and (ii) lateral extension of the terminal benzene rings with other fused arenes.[37] These techniques, used by the Haley and Tobe groups have been shown effective in tuning the OS character and aromaticity of **IF**-type scaffolds.[38] However, despite all the achievements of recent years, there are significant difficulties in predicting the electronic nature of the ground state for such diradicals since it strongly depends on spatial separation and overlapping between unpaired electrons.[30,39]

In this work, we propose a simple Ground State Stability (GSS) rule to predict the electronic ground state for a given indenofluorene-type system based on the number of Clar's π-sextets[40] it possesses in both CS and OS resonance forms. We carried out a detailed theoretical study of all the possible isomers of indenofluorene (**IF**), fluorenofluorene (**FF**), and diindenoanthracene (**DIAn**) to determine the stable ground state which allowed us to formulate and verify the GSS rule. Finally, several measures of aromaticity based on the electron density and magnetic criteria were employed to validate the proposed rule. Our concept, employing the straightforward and highly effective Clar's π-sextet model make possible the selective identification of **IF**-type systems based on their stable ground state without the need for performing advanced quantum-chemical calculations.

Computational details

Geometry optimizations for the CS isomers of the target systems were conducted using long-range corrected LC-ωPBE functional[41] with empirical (D3BJ) Grimme dispersion correction[42,43] and triple-ζ def2-TZVPP basis set.[44,45] Long-range corrected functionals provide a better description of the delocalization in π-conjugated molecules,[46–48] whereas the functionals with low percentage of HF exchange tends to exaggerate the electron delocalization.[48,49] OS structures were optimized using broken-symmetry approximation with the spin-unrestricted ULC-ωPBE-D3BJ/def2-TZVPP level of theory, as implemented in Gaussian 16 (rev. A03).[50] Normal mode vibrational frequencies were also calculated in each case to confirm the presence of local minimum, at the same level of theory. The singlet–triplet energy gap (ΔE_{S-T}) was estimated at the same level of theory.

The contribution of aromatic OS structure with the quinoidal CS resonance form was analyzed using the biradical character index (y_0) according to the Yamaguchi's scheme.[51] In addition, we used the fractional occupation number weighted density (FOD) method[52,53] to quantitatively describe the OS singlet biradical character. FOD analysis was performed with the default parameters as implemented in ORCA 4.1.2 (ref. 54) (TPSS/def2-TZVPP; T_{el} = 5000 K). Aromaticity analyses[55] were carried out based on electronic (EDDB)[56,57] and magnetic ($NICS(0)_{iso}$ and $NICS(1)_{zz}$ along with visualizing the 2D- and 3D-NICS isosurfaces)[58–61] criteria using the same level of theory. The π-electron delocalization has been also examined by the multicenter index (MCI)[62] (for details, see the ESI†).

Results and discussion

To get more insight into the electronic structure and stability of **IF**, **FF**, and **DIAn** biradicals, y_0 values, the singlet–triplet energy gap (ΔE_{S-T}), and the FOD[52] parameters were assessed. Fig. 2 demonstrates the set of the studied model compounds of **IF**, **FF**, and **DIAn** in their CS configuration with the indication of the Clar's π-sextets. To determine the extent of the multi-reference nature of the systems, the T_1 diagnostic[63] from DLPNO-CCSD(T)/cc-pVTZ single-point energy calculations[64,65] were performed for the smallest **IF** systems. Calculation revealed that in all cases T_1 values were smaller than 0.015 and 0.020 for singlet and triplet electronic states, respectively (Table S1, ESI†). Obtained number are lower than recommended T_1 diagnostics values,[63,66] therefore the systems of interest can be adequately treated using single-reference methods.

Indenofluorene family and ground state stability rule

DFT calculations reveal that all the **IF** systems have an OS ground state. In particular, **IF-1a** and **IF-2a** possess a triplet ground state with a ΔE_{S-T} gap of 2.04 and 3.65 kcal mol^{-1},

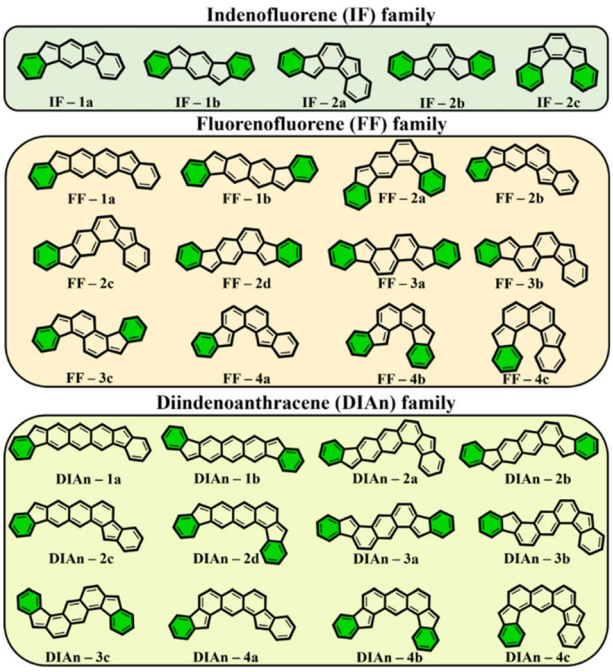

Fig. 2 The whole set of regioisomers of IF, FF, and DIAn studied in this work with their corresponding Clar's π-sextet (highlighted in green) present in the CS resonance structure.

Table 1 The calculated relative energies (kcal mol^{-1}) of isomers of **IF** in different electronic states and their computed physical parameters such as the singlet–triplet energy gap (ΔE_{S-T}), the diradical character (y_0) and the N^{FOD} values of the OS singlet state computed at the (U)LC-ωPBE/def2-TZVPP level of theory

	E (CS)	E (T)	E (OSS)	ΔE_{S-T}[a]	y_0	N^{FOD}	R[b]
IF-1a	0.00	−14.07	−12.03	2.04	0.53	1.42	1 : 3 (3)
IF-1b	0.00	13.61	−0.51	−14.12	0.03	0.68	2 : 3 (1)
IF-2a	0.00	−16.19	−12.54	3.65	1.00	2.03	1 : 3 (3)
IF-2b	0.00	8.78	−1.22	−10.00	0.07	0.94	2 : 3 (1)
IF-2c	0.00	11.91	−0.34	−12.25	0.02	0.73	2 : 3 (1)

[a] $\Delta E_{S-T} = E$ (OSS) − E (T). [b] The ratio of number of Clar's π-sextets between the ground state OS and CS resonance structures. The number in parentheses represents the spin multiplicity of this ground OS electronic state.

respectively (Table 1). Note that both structures belong to the *m*-QDM pro-aromatic network. The gain of two additional Clar's π-sextets in the OS form compared to the CS form that provides the extra stability for **IF-1a** and **IF-2a** to exist in the OS form. Previous calculations confirm that both these systems exhibit an OS ground state.[20,67] Furthermore, the mesityl-substituted **IF-1a** was studied utilizing temperature-dependent ^{1}H NMR and ESR spectroscopy, which validate the ground state to be an OS state.[22]

The obtained y_0 value of 1.00 for **IF-2a** indicates that it would exhibit pure diradical character compared to the moderate y_0 value of 0.53 for **IF-1a** (Table 1). In addition, the calculated N^{FOD} values of >1.4 for both systems (Table 1) suggest a pronounced OS character. Good agreement of y_0 and FOD values is observed since a linear relationship is often observed between them (Fig. S1, ESI†).[52] The FOD plots in Fig. S2, ESI,† show the ρ^{FOD} density is greatest on the apical carbon atom of the five-membered rings correlating the location of the radical centers in the OS structure. The calculated spin density distribution of **IF**s confirms this, showing largest amplitudes at these apical carbon atoms (Fig. S3, ESI†).

The aromaticity for the systems of interest was analyzed based on magnetic criteria using NICS(1)$_{zz}$ values for the CS and OS states respectively. In the CS singlet state of **IF-1a**, the aromatic character is prominently observed in ring A, as indicated by a NICS(1)$_{zz}$ value of −16.32 ppm, while rings B and C exhibit substantial positive values of 22.11 and 6.90 ppm, respectively, suggesting their antiaromatic nature (Fig. 3a). However, for the OS triplet state, rings A, B, and C display negative NICS(1)$_{zz}$ values, with ring A and C exhibiting relatively high negative values of −23.11 ppm, revealing the aromatic character for all three six-membered rings (Fig. 3b). In addition to the magnetic criteria, the aromaticity was analysed based on the electron density using EDDB measure of aromaticity. The calculated π-EDDB values for the OS triplet agrees well with the NICS(1)$_{zz}$ (Fig. 3), especially highlighting the aromatic character for the terminal benzene rings. This is clearly evident from the gauge-included magnetically induced currents[68–72] (GIMIC) plots, which show a diatropic current (clockwise circuit) only for a terminal benzene ring in the CS form of **IF-1a** (Fig. 3i), in contrast to the diatropic ring current observed for all six-membered rings in the OS triplet state of **IF-1a** (Fig. 3j). For these molecules, 3D-NICS$_{zz}$ maps, NICS(1)$_{zz}$ values, and ring currents lead to the same conclusions, despite the well-known fact that the contribution of shieldings from adjacent rings in some cases provides unreliable NICS results in polycyclic molecules.[72–74] The electronic and magnetic aromaticity descriptors are in good agreement with the depicted one Clar's π-sextet in the CS singlet and three Clar's π-sextets in the OS resonance structures for **IF-1a**. The same observation about the number of Clar's π-sextets can also be drawn for the **IF-2a** structure (Fig. S5, ESI†). This difference in the number of Clar's π-sextets is responsible for the relatively high stability of the OS forms for **IF-1a** and **IF-2a** structures. On the other hand, for these systems, the triplet and singlet OS species have similar energies, the triplet being slightly more stable as expected from Hund's rule.

For the other **IF** systems belonging to *p*-QDM (**IF-1b** and **IF-2c**) or *o*-QDM (**IF-2b**) networks, transition from CS to OS form is associated with an increase of only one Clar's π-sextet and thus only a modest gain in the stability observed. This, in turn, facilitates an easy return to the CS electronic state and results in a low diradical character[28,75] with a y_0 value smaller than 0.1 (Table 1), implying their categorization as nearly CS systems. Our conclusion is consistent with the previous experimental and theoretical studies,[20,28] in which the calculations also shows a y_0 value of less than 0.1 and also assigned them into a nearly CS systems.[76] However, our electronic structure calculations show that the CS singlets of these systems are slightly higher in energy than the OS singlet by 0.34 and 1.22 kcal mol^{-1} for **IF-2c** and **IF-2b**, respectively. As we said before, the OS singlet has a very low diradical character, so its energy is not much influenced by this radical character, and, therefore, a similar energy to that of the CS singlet is expected. On the other hand, the triplet state is not favored because the loss of a π-bond is not compensated by the slight increase in aromaticity. The aromaticity descriptors indicate that the terminal six-membered rings in these systems are fully Clar's π-sextet in nature for all the resonance structures (CS and OS forms). While the central benzene ring in the OS singlet state exhibits a slight enhancement in the aromaticity compared to its CS one. For instance, in the case of **IF-1b**, we can see a modest gain in the aromaticity for ring B in the OS form compared to the CS state (Fig. 3c and d).

The NICS-XY scan is useful to explore different type of ring currents in flat π-conjugated systems, especially the global and semi-global ring currents.[77,78] The NICS-XY scan (at 1.7 Å above the molecular plane) of CS state of **IF-1b** shows two diatropic rings (−17.86 ppm) at the terminal benzene rings, while the central 5–6–5 core can be considered non-aromatic. In contrast, the NICS-XY scan of the OS singlet state shows a semi-global weak diatropicity within the central 5–6–5 core with a value of −4.7 ppm (Fig. S6, ESI†). The 3D-NICS$_{zz}$ map distinctly illustrates the decrease in the deshielding region associated with the ring B in the OS state compared to the CS state. Although this increase in aromaticity cannot be attributed entirely to an additional gain of a full π-Clar's sextet ring in the OS form, it does support the presence of three aromatic rings in the OS

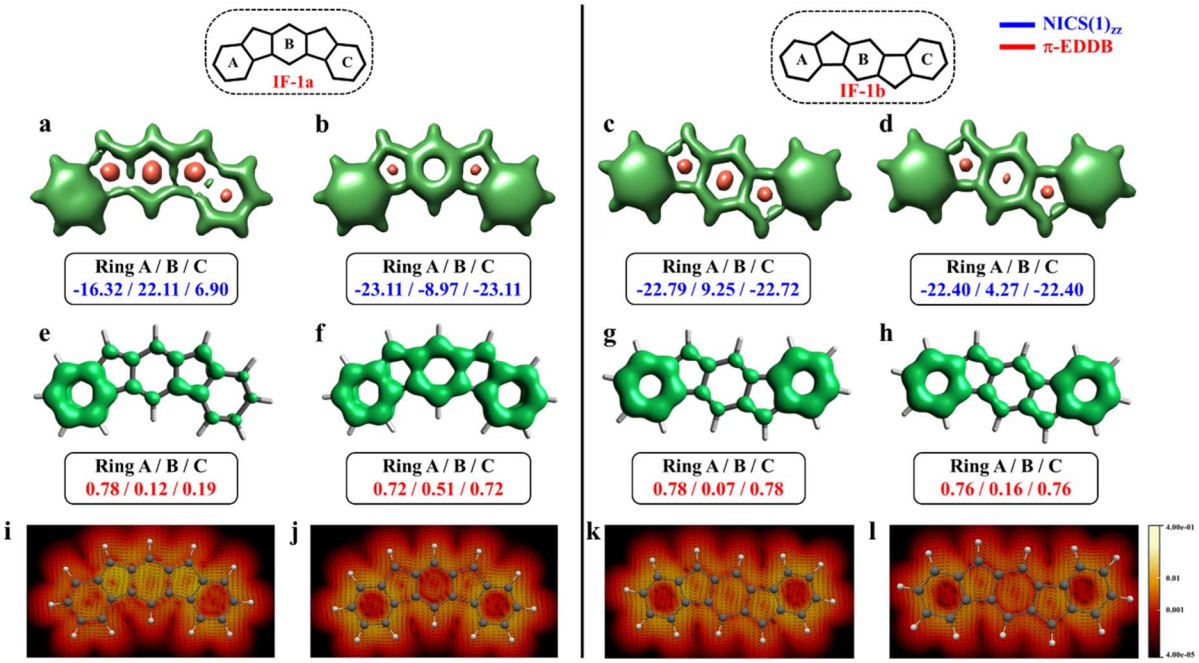

Fig. 3 3D-NICS$_{zz}$ maps (isovalues: [−15.0, 20.0]) showing shielded (green) and deshielded (salmon) regions, with NICS(1)$_{zz}$ values (blue) of six-membered rings (in ppm) for CS (a)/(c), OS triplet (b), and singlet (d) states of **IF-1a** and **IF-1b**. Also shown are π-EDDB plots (e–h) (isovalue: 0.015 e) with normalized π-EDDB values (red) and GIMIC plots (i–l) (currents in the perpendicular plane with respect to the magnetic field located 2 bohr above the molecular plane. The intensity of current decreases going from light yellow (0.4 nA T^{-1} Å^{-2}) to red and black (4 × 10^{-5} nA T^{-1} Å^{-2}), and the black arrows indicate the direction of the current flow) for the same states (see Fig. S7† for enlarged GIMIC plots).

form compared to two in the CS form. It is worth noting that the π-electron delocalization index (MCI), calculated for all **IF** systems, exhibits a similar trend to that observed with NICS and π-EDDB values (Fig. S8, ESI†). Consequently, for the analysis of aromaticity in subsequent larger systems, only NICS and EDDB criteria will be utilized. The calculated larger ΔE_{S-T} gap of −14.12 kcal mol^{-1} together with the smaller biradical character makes **IF-1b** behave nearly like a CS system. A detailed analysis of aromaticity for all the **IF**s is provided in the ESI (Fig. S4–S8, ESI†).

We utilized this difference in the number of Clar's π-sextets between the resonance structures in the CS and OS forms to determine the stability of ground state of **IF**-type systems. The proposed ground state stability (GSS) rule can be formulated as follows: "**If the OS form gains double or more the number of Clar's π-sextets compared to the CS form, the ground state of that IF-type system will be a triplet; otherwise, it will be an OS singlet**".

Validation of the GSS rule for IFs with longitudinal core extension

To make sure that the formulated GSS rule is general and can be applied to systems other than indenofluorenes, we extended the study by modifying the conjugation pathway through the extension of the core units.

We considered complete families of fluorenofluorenes (**FF**'s) and diindenoanthracenes (**DIAn**'s), in which the indene units are now linked by naphthalene and anthracene spacers respectively (Fig. 2). Similar to **IF-1a**, both **FF-1a**, and **DIAn-1a** gain more than double the number of Clar's π-sextets in the OS form compared to their corresponding CS form. In both **FF-1a** and **DIAn-1a**, the NICS(1)$_{zz}$ value for ring A in the CS form suggest an aromatic character with large negative values (−21.48 ppm for **FF-1a** and −24.35 ppm for **DIAn-1a**), whereas for ring C, they are weakly paratropic (Fig. 4a and c).

In the OS triplet form, rings A, B, and C have aromatic character, so there is a gain of two Clar's π-sextets in the OS form with respect to the CS resonance structure. In the case of **FF-1a**, the Clar's π-sextet of the OS form located in the naphthalene unit is a migrating Clar's π-sextet.[40] This gain of two Clar's π-sextets is supported by the π-EDDB and 2D-NICS(1)$_{zz}$ plots of the OS form for **FF-1a** and **DIAn-1a** structures, as depicted in Fig. S9b and d, ESI.† Therefore according to the GSS rule, both systems should possess a triplet ground state. The electronic structure calculations confirm this, showing triplet ground state with very small ΔE_{S-T} gaps (2.04 and 3.05 kcal mol^{-1} for **FF-1a** and **DIAn-1a** respectively, as shown in Table 2).

In contrast to the **FF-1a** and **DIAn-1a**, the analysis of the aromaticity for **FF-1b** and **DIAn-1b** isomers revealed that both their terminal rings exhibit pronounced aromatic character with a NICS(1)$_{zz}$ value of −24.46 and −25.35 ppm, respectively (Fig. 5). While the naphthalene spacer remains antiaromatic with a deshielded region within those rings. The transition from the CS to the OS structure induces substantial aromatization of the central ring B, while rings A and C retain almost the same level of aromaticity. The calculated π-EDDB values (Fig. 5)

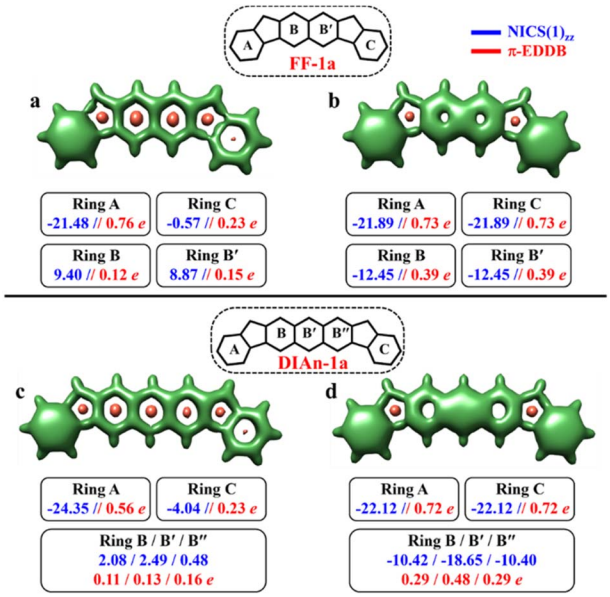

Fig. 4 3D-NICS$_{zz}$ maps showing shielded (green) and deshielded (salmon) regions, with NICS(1)$_{zz}$ (blue) and normalized π-EDDB values (red) of six-membered rings (NICS in ppm) for CS (a)/(c) and OS triplet (b)/(d) states of **FF-1a** (isovalues: [−15.0, 19.0]) and **DIAn-1a** (isovalues: [−15.0, 15.0]).

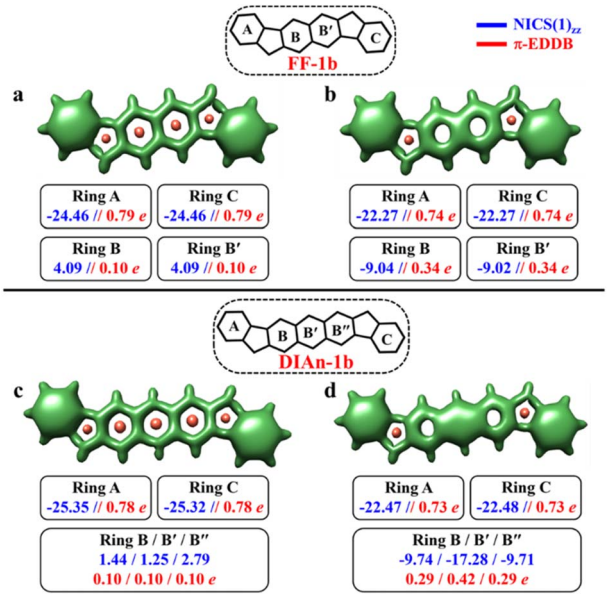

Fig. 5 3D-NICS$_{zz}$ maps showing shielded (green) and deshielded (salmon) regions, with NICS(1)$_{zz}$ (blue) and normalized π-EDDB values (red) of six-membered rings (NICS in ppm) for CS (a)/(c) and OS singlet (b)/(d) states of **FF-1b** (isovalues: [−15.0, 19.0]) and **DIAn-1b** (isovalues: [−15.0, 15.0]).

Table 2 The calculated relative energies (kcal mol^{-1}) of isomers of **FF** and **DIAn** in different electronic states and their computed physical parameters such as the singlet–triplet energy gap (ΔE_{S-T}), the diradical character (y_0) and the N^{FOD} values of the OS singlet state computed at the (U)LC-ωPBE/def2-TZVPP level of theory

	E (CS)	E (T)	E (OSS)	ΔE_{S-T}[a]	y_0	N^{FOD}	R[b]
FF-1a	0.00	−23.00	−20.96	2.04	0.69	1.55	1 : 3 (3)
FF-1b	0.00	0.30	−6.92	−7.23	0.31	1.10	2 : 3 (1)
DIAn-1a	0.00	−30.74	−27.70	3.05	0.81	1.74	1 : 3 (3)
DIAn-1b	0.00	−8.13	−13.62	−5.49	0.51	1.40	2 : 3 (1)

[a] $\Delta E_{S-T} = E$ (OSS) − E (T). [b] The ratio of number of Clar's π-sextets between the ground state OS and CS resonance structures. The number in parentheses represents the spin multiplicity of this ground OS electronic state.

together with the 2D-NICS(1)$_{zz}$ scan lead to the same conclusion (Fig. S10, ESI†). The detailed analysis of aromaticity for all the **FF** and **DIAn** systems are provided in the ESI (Fig. S9–S14, ESI†). To compare the predictions made within the GSS rule, a series of DFT calculations for the CS and OS forms of **FF-1b** and **DIAn-1b** were performed. The obtained results are in perfect agreement with the GSS rule suggesting that both **FF-1b** and **DIAn-1b** have OS singlet as their ground state. Interestingly to note that the ΔE_{S-T} gap decreases as the π-conjugation core extends from benzene (**IF-1b**) to anthracene (**DIAn-1b**), reducing from −14.12 to −5.49 kcal mol^{-1}, respectively. A notable increase in the diradical character y_0, rising from 0.03 for **IF-1b** to 0.51 for **DIAn-1b**, is also observed (Table 2). Our observations aligns with the findings from other studied diradicaloids, where elongating the conjugation distance between radical centers results in increased diradical character.[26,79] The rise in the y_0 value and the decreasing in the ΔE_{S-T} gap are linked to the increased stability of the singlet diradical state. The greater stability of the singlet state with respect to the triplet state can be rationalized by an additive dynamic spin polarization phenomenon, which stabilizes the singlet state.[29] We confirm the consistency of the GSS rule with the remaining isomers of **FF** and **DIAn** families outlined in Fig. 2. For all the examined systems, the results are in full accordance with the GSS rule: in every **IF**, **FF**, and **DIAn** isomers, if the systems acquire more than double the number of Clar's π-sextets in the OS form compared to the CS form, it adopts a triplet state; otherwise, it persists as an OS singlet state (Tables S2–S3 and Fig. S13–S14, ESI†).

Validation of the GSS rule for IFs with lateral core and outer arene ring extensions

From the previously obtained results, it is evident that longitudinal extension of the core unit from benzene (**IF**'s) to anthracene (**DIAn**'s) does not alter the applicability of the derived rule. Additionally, we explored lateral extension of the core unit in some **IF**-systems to further investigate the rule.

As illustrated in Fig. 6, the different core extensions for the **IF-2b** behave similarly to the parent system concerning the GSS rule. Specifically, the number of Clar's π-sextets in the OS resonance form is less than double compared to the CS state, indicating an OS singlet ground state. In addition, we considered several possible extensions for selected fluorenofluorenes. In particular, the core-extension applied to **FF-1a** (Fig. 6), results in more than double the number of Clar's π-sextets in the OS form compared to the CS form suggesting a triplet ground state

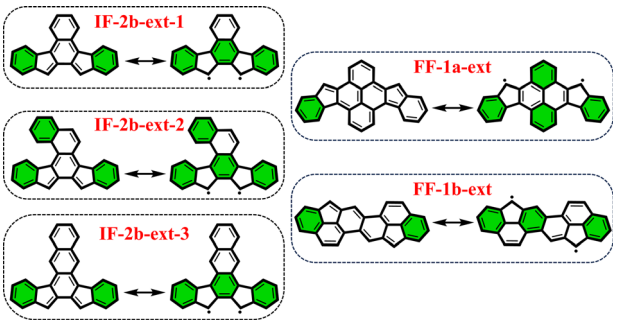

Fig. 6 Clar's π-sextet (highlighted in green) representation of some of the core-extended systems in its closed and open-shell states.

according to the GSS rule. In the literature we found an interesting example of the π-extended **FF-1b** system (**FF-1b-ext**), synthesized by Feng and co-workers[80] (Fig. 6), which involving a lateral extension that fuses the core 6-membered ring with the terminal benzene ring. According to the GSS rule this compound is expected to be an OS singlet in the electronic ground state. Indeed, our DFT calculations confirm these expectations (Table 3). All details on the aromaticity for these systems are provided in the ESI (Fig. S15–S16†).

After successfully demonstrating the GSS rule applicability to a broad type of core-extended systems, we decided to test the periphery extension. The lateral extension of the terminal benzene rings of **IF-1a** and **IF-1b** systems with π-extended (naphthalene) extremities resulted in **IF-1a-NT** and **IF-1b-NT** with increased conjugation lengths (Fig. 7).

The CS resonance form of **IF-1a-NT** allows for the depiction of one Clar's π-sextet specifically ring A (Fig. 7a), with a corresponding $NICS(1)_{zz}$ value of −23.64 ppm. In contrast, the OS form, illustrated by the 3D-$NICS_{zz}$ maps in Fig. 7b, reveals the existence of three Clar's π-sextets – rings A, B, and C with significantly greater aromaticity for the terminal rings with a $NICS(1)_{zz}$ value of −27.33 ppm. At the same time, the behavior

Table 3 The calculated relative energies (kcal mol^{-1}) of **core and periphery extended systems** in different electronic states and their computed physical parameters such as the singlet–triplet energy gap (ΔE_{S-T}), the diradical character (y_0) and the N^{FOD} values of the OS singlet state computed at the (U)LC-ωPBE/def2-TZVPP level of theory

	E (CS)	E (T)	E (OSS)	ΔE_{S-T}[a]	y_0	N^{FOD}	R[b]
Core-extension							
IF-2b-ext-1	0.00	−3.31	−9.56	−6.25	0.44	1.64	2 : 3 (1)
IF-2b-ext-2	0.00	4.07	−3.86	−7.93	0.21	1.40	2 : 3 (1)
IF-2b-ext-3	0.00	−11.33	−18.20	−6.87	0.68	2.08	2 : 3 (1)
FF-1a-ext	0.00	−44.73	−40.20	4.53	0.99	2.36	1 : 4 (3)
FF-1b-ext	0.00	2.76	−4.16	−6.93	0.25	1.12	2 : 3 (1)
Periphery-extension							
IF-1a-NT	0.00	−25.98	−21.86	4.12	0.79	1.89	1 : 3 (3)
IF-1b-NT	0.00	12.80	−0.81	−13.61	0.04	0.81	2 : 3 (1)

[a] $\Delta E_{S-T} = E$ (OSS) − E (T). [b] The ratio of number of Clar's π-sextets between the ground state OS and CS resonance structures. The number in parentheses represents the spin multiplicity of this ground OS electronic state.

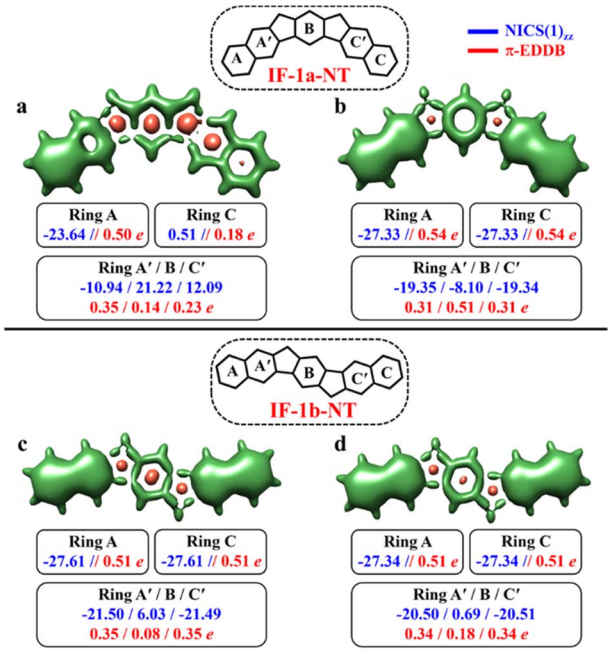

Fig. 7 3D-$NICS_{zz}$ maps showing shielded (green) and deshielded (salmon) regions, with $NICS(1)_{zz}$ (blue) and normalized π-EDDB values (red) of six-membered rings (NICS in ppm) for CS (a)/(c), OS triplet (b), and singlet (d) states of **IF-1a-NT** and **IF-1b-NT** (isovalues: [−17.5, 15.0]).

of the **IF-1b-NT** system is similar to the parental **IF-1b** – both the terminal six-membered rings in CS and OS state have a full Clar's π-sextet with a $NICS(1)_{zz}$ value of around −27.0 ppm. Most importantly in the case of ring B, $NICS(1)_{zz}$ values indicate an enhancement in the aromaticity for the OS state compared to the CS state, leading to a total of three aromatic rings in the OS form (Fig. 7d). The analysis of π-EDDB values and plots also corroborate this analysis (Fig. S17, ESI†).

As per the GSS rule, **IF-1a-NT** ground state should be a triplet, given the gain of more than double the number of Clar's π-sextet in its OS form. At the same time, **IF-1b-NT** ground state is expected to be an OS singlet, as it gains only one additional Clar's π-sextet in the OS form compared to the CS resonance form. Indeed, performed calculations confirm these predictions (Table 3). The calculations also showed a slight decrease in the ΔE_{S-T} gap for **IF-1b-NT** compared to the parent **IF-1b** by about 0.5 kcal mol^{-1}, alongside an increase in the diradical character (N^{FOD} value rising from 0.68 in **IF-1b** to 0.81 in **IF-1b-NT**).

Validation of GSS rule for IFs with massive extended and curved core

To make sure that the proposed GSS rule can be reliably used in the most sophisticated cases, involving massive core extension, we considered two systems with laterally extended anthracene spacer. Both **Coro-1a** and **Coro-1b** systems are π-extensions of **DIAn-1a** and **DIAn-1b**, respectively, and contain coronene as the core spacer (Fig. 8).

According to Clar's model, **Coro-1a** can be depicted with two Clar's π-sextets for the CS form and five for the OS form. It is

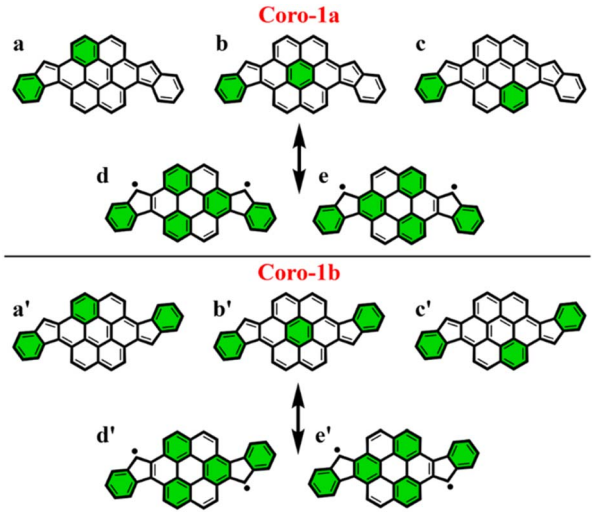

Fig. 8 Clar's π-sextet (highlighted in green) representation of **Coro-1a** and **Coro-1b** in its closed and open-shell states. (a/a′)–(c/c′) are Clar's structures for the closed-shell state and (d/d′) and (e/e′) for the open-shell state of **Coro-1a/1b**.

important to highlight that in both CS and OS forms, the Clar's model doesn't neatly align with a particular resonance structure. Instead, the valence structure of the coronene spacer is a superposition of equivalent structures and can be represented by a migrating π-sextet.[81] This is especially pronounced in the OS form, where the actual structure can be considered as a combination of two resonance structures with π-sextets that can migrate to its adjacent rings[82] (Fig. 8d and e). In accordance with the GSS rule, the ground state should be regarded as a triplet, given that transitioning from the CS to the OS form results in a gain of more than double the number of Clar's π-sextets in the CS form. Indeed, the results of quantum-chemical calculations fully support GSS rule, predicting triplet ground state with a ΔE_{S-T} gap of 3.73 kcal mol^{-1} (Table 4).

Coro-1b in contrast to **Coro-1a** structure, in the CS form, could be represented by three aromatic π-sextets – two on the terminal benzene rings and a migrating π-sextet positioned on the coronene spacer (Fig. 8a′–c′). At the same time, OS forms for **Coro-1a** and **Coro-1b** systems are the same and can be depicted by five Clar's π-sextets. Thus, according to the GSS rule **Coro-1b** should exhibit an OS singlet ground state, since the number of Clar's π-sextets in the OS form is less than double the number of Clar's π-sextets in the CS form. The DFT calculations confirm that the ground state in **Coro-1b** is an OS singlet, with a ΔE_{S-T} gap of −3.80 kcal mol^{-1}. It is worth noting that **Coro-1a** and **Coro-1b**, which have an OS singlet state of similar diradical character, have different states as their ground states.

As seen in Fig. 9, the 3D-NICS$_{zz}$ map illustrates the difference in aromaticity for the terminal benzene rings between **Coro-1a** and **Coro-1b** in the CS state. As expected, the migrating Clar's π-sextet in the coronene spacer is evident from these plots (Fig. 9a and c), as well as from the provided NICS(1)$_{zz}$ values. Meanwhile, in the OS form, the NICS(1)$_{zz}$ values for the benzene rings in the coronene spacer exhibit very similar values for both **Coro-1a** and **Coro-1b** structures, indicating the delocalized nature of the spacer. This is supported by the aromaticity analysis using the electronic descriptor π-EDDB values (Fig. 9), 2D-NICS(1)$_{zz}$, and π-EDDB plots (Fig. S18, ESI†).

It is worth mentioning that Kubo *et al.* demonstrated that in benzenoid CPHs with the same chemical composition, the molecule with more aromatic Clar's π-sextets in the diradical resonance forms has greater diradical character.[83,84] While this

Table 4 The calculated relative energies (kcal mol^{-1}) of **Coro-1a/1b** and **Coro-1a/1b** in different electronic states and their computed physical parameters such as the singlet–triplet energy gap (ΔE_{S-T}), the diradical character (y_0) and the N^{FOD} values of the OS singlet state computed at the (U)LC-ωPBE/def2-TZVPP level of theory

	E (CS)	E (T)	E (OSS)	ΔE_{S-T}[a]	y_0	N^{FOD}	R[b]
Coro-1a	0.00	−38.30	−34.57	3.73	0.94	2.24	2 : 5 (3)
Coro-1b	0.00	−17.89	−21.69	−3.80	0.75	2.04	3 : 5 (1)
Cora-1a	0.00	−39.88	−39.06	0.82	0.98	2.40	2 : 4 (3)
Cora-1b	0.00	−28.80	−27.30	1.51	0.94	2.26	2 : 4 (3)

[a] $\Delta E_{S-T} = E$ (OSS) − E (T). [b] The ratio of number of Clar's π-sextets between the ground state OS and CS resonance structures. The number in parentheses represents the spin multiplicity of this ground OS electronic state.

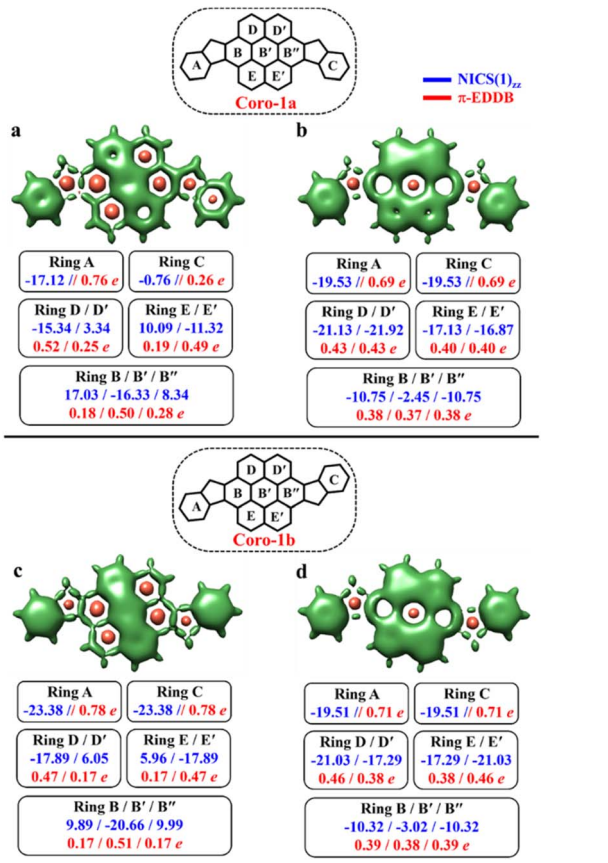

Fig. 9 3D-NICS$_{zz}$ maps showing shielded (green) and deshielded (salmon) regions, with NICS(1)$_{zz}$ (blue) and normalized π-EDDB values (red) of six-membered rings (NICS in ppm) for CS (a)/(c), OS triplet (b) and singlet (d) states of **Coro-1a** and **Coro-1b** (isovalues: [−17.5, 15.0]).

rule is interesting, our study uses the ratio of Clar's π-sextets in CS and OS forms instead of the difference in their numbers. To explain this, we compared two sets of molecules: **DIAn-1a**/**1b** and **Coro-1a**/**1b**. The **Coro-1a**/**1b** systems gain more Clar's π-sextets when transitioning to OS states (3 and 2, respectively) compared to the **DIAn-1a**/**1b** systems (2 and 1, respectively). However, the increase in global aromaticity is smaller for **Coro** systems than for **DIAn** systems (Table S4, ESI†). This means that simply counting the gain in Clar's π-sextets is not a reliable way to predict the preferred electronic state. Instead, we found that the ratio of Clar's π-sextets between CS and OS states is a more consistent and reliable predictor across different systems, regardless of the size of the π-electron system.

To further explore the applicability of the GSS rule we examined two, not just core-extended, but also bent systems. Both these regioisomers – **Cora-1a** and **Cora-1b**, that can be considered as **IF**-type systems with corannulene spacers, were synthesized and characterized by Cao and co-workers (Fig. 10).[85]

According to the Clar's model, both the **Cora-1a** and **Cora-1b** can be represented as having two Clar's π-sextets, comprising the terminal benzene rings in the CS form. Additionally, the CS form of **Cora-1b** can also be represented by two other resonance structures (Fig. 10a″ and a‴), where one Clar's π-sextet resides on the terminal benzene ring and the other within the corannulene spacer. However, in the case of the OS form, both **Cora-1a** and **Cora-1b** exhibit four Clar's π-sextets – two in the terminal benzene rings and the other two as migrating sextets within the corannulene spacer (Fig. 10). Therefore, in line with the GSS rule, with the doubling of the number of Clar's π-sextets in the OS form compared to the CS form, both systems should be in a triplet ground state. Indeed, our DFT calculations fully support this, predicting a triplet as the ground state with a small ΔE_{S-T} gap of 0.82 and 1.51 kcal mol^{-1} for **Cora-1a** and **Cora-1b**, respectively (Table 4). The calculated diradical character of more than 0.94 for both systems suggests they are nearly pure diradicals consistent with reported values.[85]

As depicted in Fig. 11, the NICS(0)$_{iso}$ values suggest the difference in aromaticity for the terminal benzene rings between **Cora-1a** and **Cora-1b** in the CS state. In **Cora-1a**, both terminal benzene rings, ring A and C provide a NICS(1)$_{zz}$ value of −17.22 ppm, whereas in **Cora-1b**, the most aromatic rings correspond to terminal ring C and ring D from the corannulene spacer, with a value exceeding −18.94 ppm. Consequently, resonance structure a‴ (Fig. 10) corresponds to the CS form of **Cora-1b** according to the aromaticity analysis. Meanwhile in the OS form, there is an increase in aromaticity for both systems. Specifically, both **Cora-1a** and **Cora-1b** shows pronounced

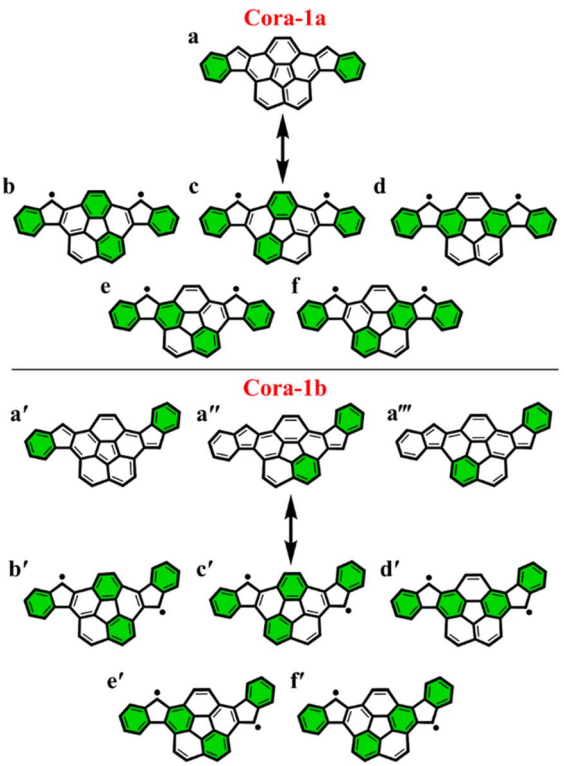

Fig. 10 Clar's π-sextet (highlighted in green) representation of **Cora-1a** and **Cora-1b** in its closed and open-shell states. For **Cora-1a**, (a) is the Clar's representation of the closed-shell state and a combination of (b–f) is the Clar's representation of the open-shell state. For **Cora-1b**, the combination of (a′, a″ and a‴) is the Clar's representation of the closed-shell state and a combination of (b′–f′) is the Clar's representation of the open-shell state.

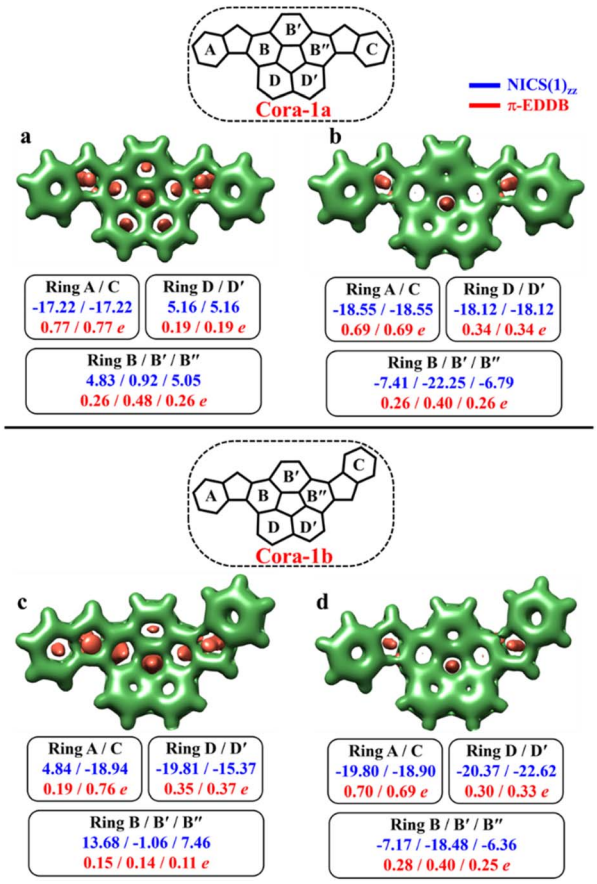

Fig. 11 3D-NICS$_{iso}$ maps showing shielded (green) and deshielded (salmon) regions, with NICS(1)$_{zz}$ (blue) and normalized π-EDDB values (red) of six-membered rings (NICS in ppm) for CS (a)/(c) and OS triplet (b)/(d) states of **Cora-1a** and **Cora-1b** (isovalues: [−11.0, 0.0]).

aromatic character in both terminal rings (with NICS(1)$_{zz}$ values ranging from −18.5 to −19.8 ppm) and two other rings from the corannulene spacer (values ranging from −18.1 to −22.6 ppm), suggesting a greater contribution from resonance structures b/c and b′/c′ (Fig. 10) for **Cora-1a** and **Cora-1b**, respectively. These trends are also evident in the π-EDDB values and plots (Fig. S19, ESI†). This result further validates the GSS rule with the presence of two and four Clar's π-sextets in the CS and OS forms of these systems.

Exploring the GSS rule beyond IF systems

In order to test the applicability of the proposed GSS rule to systems beyond the **IF**-type, several biradicaloids that are polycyclic arenes have been selected. Among the tested systems, we considered heptazethrene (**HPZ1** and **HPZ2**)[86,87] and octazethrene (**OCZ**)[88] derivatives, benzo-extended bis-periazulene (**BPaz**),[89,90] and azulene-embedded nanographene (**Az-NG**)[91] (Fig. 12).

As seen, the selected biradicaloids have different ratios of the Clar's π-sextets in their CS and OS states and thus, in accordance with the GSS rule, must appear either as OS singlets or as triplets. In the case of **HPZ1**, **HPZ2**, **OCZ**, and **Az-NG**, the ratio of Clar's π-sextets is less than two; thus, these systems are expected to be OS singlets in their ground state. For **BPaz**, the ratio is equal to three, and thus a triplet state must be the ground state. Performed quantum chemical calculations (see Table 5) fully confirmed the correctness of the predictions made within the GSS rule.

As can be noticed, in the majority of considered cases, the difference in Clar's π-sextet numbers between the CS and the corresponding OS electronic state follows a certain pattern (see Table S5†). In particular, if there is a gain of more than one Clar's π-sextet in the OS form compared to the CS form, the ground state of that **IF**-type system will be a triplet; otherwise, it will be an OS singlet.[92] Indeed, the rule formulated in this way works well for parental **IF**-, **FF**-, and **DIAn**-systems. Moreover, lateral core extension and outer arene ring extension do not lead to its violation. However, for massively core-extended systems like **Coro-1b**, the rule formulated in terms of the difference in Clar's π-sextets gives an incorrect prediction. Another system in which the ground state does not correspond to predictions made on the basis of the difference in the number of Clar's π-sextets is **Az-NG**. Note that in both mentioned cases, the difference between OS singlet and triplet states was found to be −3.80 and −1.64 kcal mol^{-1} for **Coro-1b** and **Az-NG**, respectively. These values are rather small and can potentially be rationalized by the non-accounting of a resonance term of the Clar's resonators[81,92] (Fig. S20, ESI†). A comparison of the difference in Clar's π-sextet numbers and their ratio for all studied systems is provided in Table S5, ESI.† It is important to highlight that the proposed GSS rule, which uses the ratio of number of Clar's π-sextets between the CS and OS states instead of the difference in their exact numbers, accurately predicts the ground state for all the studied systems without any exceptions.

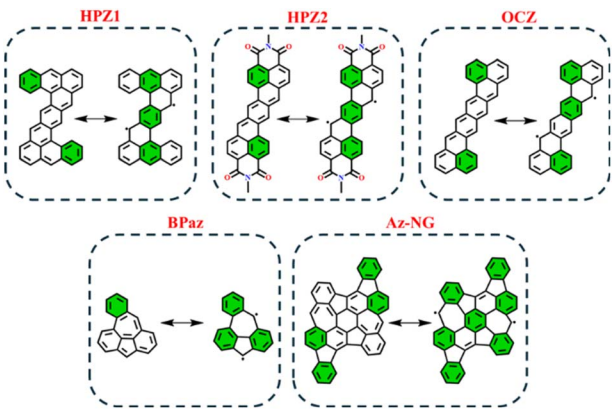

Fig. 12 Graphical representation of non-indenofluorene-type biradicaloids in their closed and open-shell states. Clar's π-sextet is highlighted in green.

Table 5 The calculated relative energies (kcal mol^{-1}) of selected non-indenofluorene-type biradicaloids in different electronic states and their computed physical parameters such as the singlet–triplet energy gap (ΔE_{S-T}), the diradical character (y_0), and the N^{FOD} values of the OS singlet state computed at the (U)LC-ωPBE/def2-TZVPP level of theory

	E (CS)	E (T)	E (OSS)	ΔE_{S-T}[a]	y_0	N^{FOD}	R[b]
HPZ1	0.00	−2.44	−11.78	−9.34	0.45	1.53	2 : 3 (1)
HPZ2	0.00	−0.33	−9.44	−9.11	0.38	1.53	2 : 3 (1)
OCZ	0.00	−5.80	−14.37	−8.58	0.50	1.50	2 : 3 (1)
Az-NG	0.00	−19.48	−21.12	−1.64	0.82	2.27	4 : 7 (1)
BPaz	0.00	−13.16	−7.65	5.51	0.65	1.54	1 : 3 (3)

[a] $\Delta E_{S-T} = E$ (OSS) − E (T). [b] The ratio of number of Clar's π-sextets between the ground state OS and CS resonance structures. The number in parentheses represents the spin multiplicity of this ground OS electronic state.

Overall, the excellent performance of the GSS rule in predicting the nature of the ground state not only in **IF**-type systems but also in other arene biradicals confirms that the proposed rule is reliable and robust and can be applied to a wide variety of organic systems. Finally, for all the studied system, the comparison of global aromaticity in both CS and corresponding OS electronic states shows that OS states (both triplet and singlet biradical) exhibit higher aromaticity compared to CS states (Table S4, ESI†). Notably, the increase in aromaticity is more pronounced in the triplet state than in the OS singlet state. This observation aligns with the increase in the number of Clar's π-sextets during the transition from CS to OS forms.

Conclusions

In this work, we formulate a simple rule to predict the ground state stability of a class of indenofluorene-type systems based on the number of Clar's π-sextets present in their closed-shell and open-shell resonance structures. The complete set of isomers, beginning from the indenofluorene (**IF**) featuring a single six-membered ring core, as well as their longitudinally π-extended version with naphthalene (**FF**) and anthracene (**DIAn**) between two indene units were considered for the proposed rule validation. Moreover, selected systems with π-extended terminal rings and laterally extended core spacers were also examined.

In accordance with the proposed GSS rule, the electronic ground state of the **IF**-type system is triplet if there is a gain of double or more the number of Clar's π-sextets in the open-shell resonance form compared to the closed-shell form; otherwise, the ground state is an open-shell singlet. Performed quantum chemical calculations and analysis of the aromaticity of studied systems confirms the proposed rule and demonstrates that aromaticity plays the most crucial role in determining of the electronic ground state for such polycyclic hydrocarbons. The simplicity of the GSS rule together with the underlying Clar's π-sextet model makes the proposed rule a powerful and easy-to-use tool for selecting systems with desirable properties for building new **IF**-type materials.

Data availability

The detailed description of the supporting data included in the ESI,† which contains relative energies in different electronic states for all the studied systems and the detailed analysis of aromaticity for the same. The results of the DFT simulations for the systems of interest are available at **https://doi.org/10.5281/zenodo.12532666**.

Author contributions

G. G. investigation, data curation, formal analysis, writing – original draft, writing – review & editing. A. J. S. investigation, supervision, writing – review & editing. M. S. supervision, writing – review & editing, funding acquisition.

Conflicts of interest

There are no conflicts to declare.

Acknowledgements

We are grateful for financial support from the Spanish Ministerio de Ciencia e Innovación (Network RED2018-102815-T, project PID2020-113711GB-I00/MCIN/AEI/10.13039/501100011033), and the Catalan Conselleria de Recerca i Universitats of the Generalitat de Catalunya (project 2021SGR623). G. G. is thankful for the contract 2020 FISDU 00345 from the Generalitat de Catalunya. A. J. S. gratefully acknowledges Poland's high-performance computing infrastructure PLGrid (HPC Centers: ACK Cyfronet AGH) for providing computer facilities and support within computational grant no. PLG/2022/015981 and PLG/2023/016841. Authors are grateful to Consorci de Serveis Universitaris de Catalunya (CSUC) for the computational time.

References

1 Z. Zeng, Y. M. Sung, N. Bao, D. Tan, R. Lee, J. L. Zafra, B. S. Lee, M. Ishida, J. Ding, J. T. López Navarrete, Y. Li, W. Zeng, D. Kim, K.-W. Huang, R. D. Webster, J. Casado and J. Wu, *J. Am. Chem. Soc.*, 2012, **134**, 14513–14525.
2 L. Zhang, Y. Cao, N. S. Colella, Y. Liang, J.-L. Brédas, K. N. Houk and A. L. Briseno, *Acc. Chem. Res.*, 2015, **48**, 500–509.
3 D. M. Guldi, B. M. Illescas, C. M. Atienza, M. Wielopolski and N. Martín, *Chem. Soc. Rev.*, 2009, **38**, 1587–1597.
4 M. Hermann, D. Wassy and B. Esser, *Angew. Chem., Int. Ed.*, 2021, **60**, 15743–15766.
5 V. A. Dediu, L. E. Hueso, I. Bergenti and C. Taliani, *Nat. Mater.*, 2009, **8**, 707–716.
6 Y. Morita, S. Nishida, T. Murata, M. Moriguchi, A. Ueda, M. Satoh, K. Arifuku, K. Sato and T. Takui, *Nat. Mater.*, 2011, **10**, 947–951.
7 J. M. Fernández-García, P. J. Evans, S. Filippone, M. Á. Herranz and N. Martín, *Acc. Chem. Res.*, 2019, **52**, 1565–1574.
8 S. Mishra, G. Catarina, F. Wu, R. Ortiz, D. Jacob, K. Eimre, J. Ma, C. A. Pignedoli, X. Feng, P. Ruffieux, J. Fernández-Rossier and R. Fasel, *Nature*, 2021, **598**, 287–292.
9 C. Poriel and J. Rault-Berthelot, *Chem. Soc. Rev.*, 2023, **52**, 6754–6805.
10 D. Kong, T. Cai, H. Fan, H. Hu, X. Wang, Y. Cui, D. Wang, Y. Wang, H. Hu, M. Wu, Q. Xue, Z. Yan, X. Li, L. Zhao and W. Xing, *Angew. Chem., Int. Ed.*, 2022, **61**, e202114681.
11 M. D. Hager, B. Esser, X. Feng, W. Schuhmann, P. Theato and U. S. Schubert, *Adv. Mater.*, 2020, **32**, 2000587.
12 P. Hu, S. Lee, T. S. Herng, N. Aratani, T. P. Gonçalves, Q. Qi, X. Shi, H. Yamada, K.-W. Huang, J. Ding, D. Kim and J. Wu, *J. Am. Chem. Soc.*, 2016, **138**, 1065–1077.
13 J. E. Anthony, *Chem. Rev.*, 2006, **106**, 5028–5048.
14 Z. Majzik, N. Pavliček, M. Vilas-Varela, D. Pérez, N. Moll, E. Guitián, G. Meyer, D. Peña and L. Gross, *Nat. Commun.*, 2018, **9**, 1198.
15 G. Merino, M. Solà, I. Fernández, C. Foroutan-Nejad, P. Lazzeretti, G. Frenking, H. L. Anderson, D. Sundholm, F. P. Cossío, M. A. Petrukhina, J. Wu, J. I. Wu and A. Restrepo, *Chem. Sci.*, 2023, **14**, 5569–5576.
16 C. K. Frederickson, B. D. Rose and M. M. Haley, *Acc. Chem. Res.*, 2017, **50**, 977–987.
17 S. Mishra, M. Vilas-Varela, L.-A. Lieske, R. Ortiz, S. Fatayer, I. Rončević, F. Albrecht, T. Frederiksen, D. Peña and L. Gross, *Nat. Chem.*, 2024, **16**, 755–761.
18 D. T. Chase, B. D. Rose, S. P. McClintock, L. N. Zakharov and M. M. Haley, *Angew. Chem., Int. Ed.*, 2011, **50**, 1127–1130.
19 A. G. Fix, P. E. Deal, C. L. Vonnegut, B. D. Rose, L. N. Zakharov and M. M. Haley, *Org. Lett.*, 2013, **15**, 1362–1365.
20 J. J. Dressler, Z. Zhou, J. L. Marshall, R. Kishi, S. Takamuku, Z. Wei, S. N. Spisak, M. Nakano, M. A. Petrukhina and M. M. Haley, *Angew. Chem., Int. Ed.*, 2017, **56**, 15363.
21 A. Shimizu and Y. Tobe, *Angew. Chem., Int. Ed.*, 2011, **50**, 6906–6910.
22 A. Shimizu, R. Kishi, M. Nakano, D. Shiomi, K. Sato, T. Takui, I. Hisaki, M. Miyata and Y. Tobe, *Angew. Chem., Int. Ed.*, 2013, **52**, 6076–6079.
23 E. Clar and R. Schoental, *Polycyclic hydrocarbons*, Springer-Verlag, Berlin, 1964, vol. 2.
24 E. Clar, *The Aromatic Sextet*, New York, Wiley, 1972.

25 L. K. Montgomery, J. C. Huffman, E. A. Jurczak and M. P. Grendze, *J. Am. Chem. Soc.*, 1986, **108**, 6004–6011.
26 S. Escayola, M. Callís, A. Poater and M. Solà, *ACS Omega*, 2019, **4**, 10845–10853.
27 K. Yamaguchi, *Chem. Phys. Lett.*, 1975, **33**, 330–335.
28 M. Di Giovannantonio, K. Eimre, A. V Yakutovich, Q. Chen, S. Mishra, J. I. Urgel, C. A. Pignedoli, P. Ruffieux, K. Müllen, A. Narita and R. Fasel, *J. Am. Chem. Soc.*, 2019, **141**, 12346–12354.
29 P. Karafiloglou, *J. Chem. Educ.*, 1989, **66**, 816.
30 M. Abe, *Chem. Rev.*, 2013, **113**, 7011–7088.
31 I. Badía-Domínguez, S. Canola, V. Hernández Jolín, J. T. López Navarrete, J. C. Sancho-García, F. Negri and M. C. Ruiz Delgado, *J. Phys. Chem. Lett.*, 2022, **13**, 6003–6010.
32 C. A. Barboza, R. Bast, E. Barboza, D. MacLeod-Carey and R. Arratia-Perez, *New J. Chem.*, 2018, **42**, 15648–15654.
33 B. D. Rose, C. L. Vonnegut, L. N. Zakharov and M. M. Haley, *Org. Lett.*, 2012, **14**, 2426–2429.
34 J. E. Barker, C. K. Frederickson, M. H. Jones, L. N. Zakharov and M. M. Haley, *Org. Lett.*, 2017, **19**, 5312–5315.
35 A. S. Hacker, M. Pavano, J. E. Wood, H. Hashimoto, K. M. D'Ambrosio, C. K. Frederickson, J. L. Zafra, C. J. Gómez-García, V. Postils, A. Ringer McDonald, D. Casanova, D. K. Frantz and J. Casado, *Chem. Commun.*, 2019, **55**, 14186–14189.
36 G. E. Rudebusch, J. L. Zafra, K. Jorner, K. Fukuda, J. L. Marshall, I. Arrechea-Marcos, G. L. Espejo, R. Ponce Ortiz, C. J. Gómez-García, L. N. Zakharov, M. Nakano, H. Ottosson, J. Casado and M. M. Haley, *Nat. Chem.*, 2016, **8**, 753–759.
37 J. J. Dressler and M. M. Haley, *J. Phys. Org. Chem.*, 2020, **33**, e4114.
38 J. Guo, X. Tian, Y. Wang and C. Dou, *Chem. Res. Chin. Univ.*, 2023, **39**, 161–169.
39 X. Xu, S. Takebayashi, H. Hanayama, S. Vasylevskyi, T. Onishi, T. Ohto, H. Tada and A. Narita, *J. Am. Chem. Soc.*, 2023, **145**, 3891–3896.
40 M. Solà, *Front. Chem.*, 2013, **1**, 22.
41 O. A. Vydrov and G. E. Scuseria, *J. Chem. Phys.*, 2006, **125**, 234109.
42 S. Grimme, S. Ehrlich and L. Goerigk, *J. Comput. Chem.*, 2011, **32**, 1456–1465.
43 S. Grimme, J. Antony, S. Ehrlich and H. Krieg, *J. Chem. Phys.*, 2010, **132**, 154104.
44 O. A. Vydrov, J. Heyd, A. V Krukau and G. E. Scuseria, *J. Chem. Phys.*, 2006, **125**, 74106.
45 F. Weigend and R. Ahlrichs, *Phys. Chem. Chem. Phys.*, 2005, **7**, 3297–3305.
46 D. W. Szczepanik, M. Solà, M. Andrzejak, B. Pawełek, J. Dominikowska, M. Kukułka, K. Dyduch, T. M. Krygowski and H. Szatylowicz, *J. Comput. Chem.*, 2017, **38**, 1640–1654.
47 I. Casademont-Reig, T. Woller, J. Contreras-García, M. Alonso, M. Torrent-Sucarrat and E. Matito, *Phys. Chem. Chem. Phys.*, 2018, **20**, 2787–2796.
48 L. J. Karas, S. Jalife, R. V Viesser, J. V Soares, M. M. Haley and J. I. Wu, *Angew. Chem., Int. Ed.*, 2023, **62**, e202307379.
49 R. A. King, T. D. Crawford, J. F. Stanton and H. F. Schaefer, *J. Am. Chem. Soc.*, 1999, **121**, 10788–10793.
50 M. J. Frisch, G. W. Trucks, H. B. Schlegel, G. E. Scuseria, M. A. Robb, J. R. Cheeseman, G. Scalmani, V. Barone, G. A. Petersson, H. Nakatsuji, X. Li, M. Caricato, A. V. Marenich, J. Bloino, B. G. Janesko, R. Gomperts, B. Mennucci, H. P. Hratchian, J. V. Ortiz, A. F. Izmaylov, J. L. Sonnenberg, D. Williams-Young, F. Ding, F. Lipparini, F. Egidi, J. Goings, B. Peng, A. Petrone, T. Henderson, D. Ranasinghe, V. G. Zakrzewski, J. Gao, N. Rega, G. Zheng, W. Liang, M. Hada, M. Ehara, K. Toyota, R. Fukuda, J. Hasegawa, M. Ishida, T. Nakajima, Y. Honda, O. Kitao, H. Nakai, T. Vreven, K. Throssell, J. A. Montgomery Jr, J. E. Peralta, F. Ogliaro, M. J. Bearpark, J. J. Heyd, E. N. Brothers, K. N. Kudin, V. N. Staroverov, T. A. Keith, R. Kobayashi, J. Normand, K. Raghavachari, A. P. Rendell, J. C. Burant, S. S. Iyengar, J. Tomasi, M. Cossi, J. M. Millam, M. Klene, C. Adamo, R. Cammi, J. W. Ochterski, R. L. Martin, K. Morokuma, O. Farkas, J. B. Foresman and D. J. Fox, *Gaussian 16, Revision A.03*, Gaussian, Inc., Wallingford, 2016.
51 K. Yamaguchi, F. Jensen, A. Dorigo and K. N. Houk, *Chem. Phys. Lett.*, 1988, **149**, 537–542.
52 C. A. Bauer, A. Hansen and S. Grimme, *Chem.–Eur. J.*, 2017, **23**, 6150–6164.
53 S. Grimme and A. Hansen, *Angew. Chem., Int. Ed.*, 2015, **54**, 12308–12313.
54 F. Neese, *Wiley Interdiscip. Rev.: Comput. Mol. Sci.*, 2012, **2**, 73–78.
55 M. Solà, A. I. Boldyrev, M. K. Cyrañski, T. M. Krygowski and G. Merino, *Aromaticity and Antiaromaticity: Concepts and Applications*, Wiley, Chichester, 2022.
56 D. W. Szczepanik, M. Andrzejak, K. Dyduch, E. Żak, M. Makowski, G. Mazur and J. Mrozek, *Phys. Chem. Chem. Phys.*, 2014, **16**, 20514–20523.
57 D. W. Szczepanik, M. Andrzejak, J. Dominikowska, B. Pawełek, T. M. Krygowski, H. Szatylowicz and M. Solà, *Phys. Chem. Chem. Phys.*, 2017, **19**, 28970–28981.
58 I. Fernández, *Aromaticity: Modern Computational Methods and Applications*, Elsevier, Dordretch, 2021.
59 P. v. R. Schleyer, C. Maerker, A. Dransfeld, H. Jiao and N. J. R. van Eikema Hommes, *J. Am. Chem. Soc.*, 1996, **118**, 6317–6318.
60 R. Gershoni-Poranne and A. Stanger, *Chem.–Eur. J.*, 2014, **20**, 5673–5688.
61 E. Kleinpeter and A. Koch, *Org. Biomol. Chem.*, 2024, **22**, 3035–3044.
62 P. Bultinck, R. Ponec and S. Van Damme, *J. Phys. Org. Chem.*, 2005, **18**, 706–718.
63 T. J. Lee and P. R. Taylor, *Int. J. Quantum Chem.*, 1989, **36**, 199–207.
64 J. Noga and R. J. Bartlett, *J. Chem. Phys.*, 1987, **86**, 7041–7050.
65 T. H. Dunning Jr., *J. Chem. Phys.*, 1989, **90**, 1007–1023.
66 R. Meana-Pañeda, X. Xu, H. Ma and D. G. Truhlar, *J. Phys. Chem. A*, 2017, **121**, 1693–1707.
67 J. E. Barker, J. J. Dressler, A. Cárdenas Valdivia, R. Kishi, E. T. Strand, L. N. Zakharov, S. N. MacMillan, C. J. Gómez-

García, M. Nakano, J. Casado and M. M. Haley, *J. Am. Chem. Soc.*, 2020, **142**, 1548–1555.
68 H. Fliegl, S. Taubert, O. Lehtonen and D. Sundholm, *Phys. Chem. Chem. Phys.*, 2011, **13**, 20500–20518.
69 D. Sundholm, R. J. F. Berger and H. Fliegl, *Phys. Chem. Chem. Phys.*, 2016, **18**, 15934–15942.
70 M. Orozco-Ic and G. Merino, *Chemistry*, 2021, **3**, 1381–1391.
71 E. Paenurk and R. Gershoni-Poranne, *Phys. Chem. Chem. Phys.*, 2022, **24**, 8631–8644.
72 M. Orozco-Ic, M. Dimitrova, J. Barroso, D. Sundholm and G. Merino, *J. Phys. Chem. A*, 2021, **125**, 5753–5764.
73 D. Inostroza, V. García, O. Yañez, J. J. Torres-Vega, A. Vásquez-Espinal, R. Pino-Rios, R. Báez-Grez and W. Tiznado, *New J. Chem.*, 2021, **45**, 8345–8351.
74 J. Poater, M. Solà, R. G. Viglione and R. Zanasi, *J. Org. Chem.*, 2004, **69**, 7537–7542.
75 S. Moles Quintero, M. M. Haley, M. Kertesz and J. Casado, *Angew. Chem., Int. Ed.*, 2022, **61**, e202209138.
76 K. Fukuda, T. Nagami, J. Fujiyoshi and M. Nakano, *J. Phys. Chem. A*, 2015, **119**, 10620–10627.
77 A. Stanger, G. Monaco and R. Zanasi, *ChemPhysChem*, 2020, **21**, 65–82.
78 J. L. Marshall, K. Uchida, C. K. Frederickson, C. Schütt, A. M. Zeidell, K. P. Goetz, T. W. Finn, K. Jarolimek, L. N. Zakharov, C. Risko, R. Herges, O. D. Jurchescu and M. M. Haley, *Chem. Sci.*, 2016, **7**, 5547–5558.
79 P. Hu and J. Wu, *Can. J. Chem.*, 2016, **95**, 223–233.
80 J. Liu, J. Ma, K. Zhang, P. Ravat, P. Machata, S. Avdoshenko, F. Hennersdorf, H. Komber, W. Pisula, J. J. Weigand, A. A. Popov, R. Berger, K. Müllen and X. Feng, *J. Am. Chem. Soc.*, 2017, **139**, 7513–7521.
81 Y. Wang, *J. Phys. Chem. A*, 2022, **126**, 164–176.
82 A. Kumar, M. Duran and M. Solà, *J. Comput. Chem.*, 2017, **38**, 1606–1611.
83 S. Das and J. Wu, in *Polycyclic Arenes and Heteroarenes*, Wiley-VCH, Weinheim, 2015, pp. 1–36.
84 A. Konishi, Y. Hirao, M. Nakano, A. Shimizu, E. Botek, B. Champagne, D. Shiomi, K. Sato, T. Takui, K. Matsumoto, H. Kurata and T. Kubo, *J. Am. Chem. Soc.*, 2010, **132**, 11021–11023.
85 R.-Q. Lu, S. Wu, L.-L. Yang, W.-B. Gao, H. Qu, X.-Y. Wang, J.-B. Chen, C. Tang, H.-Y. Shi and X.-Y. Cao, *Angew. Chem., Int. Ed.*, 2019, **58**, 7600–7605.
86 Z. Sun, S. Lee, K. H. Park, X. Zhu, W. Zhang, B. Zheng, P. Hu, Z. Zeng, S. Das, Y. Li, C. Chi, R.-W. Li, K.-W. Huang, J. Ding, D. Kim and J. Wu, *J. Am. Chem. Soc.*, 2013, **135**, 18229–18236.
87 Z. Sun, K.-W. Huang and J. Wu, *J. Am. Chem. Soc.*, 2011, **133**, 11896–11899.
88 Y. Li, W.-K. Heng, B. S. Lee, N. Aratani, J. L. Zafra, N. Bao, R. Lee, Y. M. Sung, Z. Sun, K.-W. Huang, R. D. Webster, J. T. López Navarrete, D. Kim, A. Osuka, J. Casado, J. Ding and J. Wu, *J. Am. Chem. Soc.*, 2012, **134**, 14913–14922.
89 K. Horii, R. Kishi, M. Nakano, D. Shiomi, K. Sato, T. Takui, A. Konishi and M. Yasuda, *J. Am. Chem. Soc.*, 2022, **144**, 3370–3375.
90 F. Wu, J. Ma, F. Lombardi, Y. Fu, F. Liu, Z. Huang, R. Liu, H. Komber, D. I. Alexandropoulos, E. Dmitrieva, T. G. Lohr, N. Israel, A. A. Popov, J. Liu, L. Bogani and X. Feng, *Angew. Chem., Int. Ed.*, 2022, **61**, e202202170.
91 J. Liu, S. Mishra, C. A. Pignedoli, D. Passerone, J. I. Urgel, A. Fabrizio, T. G. Lohr, J. Ma, H. Komber, M. Baumgarten, C. Corminboeuf, R. Berger, P. Ruffieux, K. Müllen, R. Fasel and X. Feng, *J. Am. Chem. Soc.*, 2019, **141**, 12011–12020.
92 This alternative formulation was proposed by Reviewer 1.